The signaling lipid PI(3,5)P_2 stabilizes V_1–V_o sector interactions and activates the V-ATPase

Sheena Claire Li[a], Theodore T. Diakov[a], Tao Xu[b], Maureen Tarsio[a], Wandi Zhu[a], Sergio Couoh-Cardel[a], Lois S. Weisman[b], and Patricia M. Kane[a]

[a]Department of Biochemistry and Molecular Biology, SUNY Upstate Medical University, Syracuse, NY 13219; [b]Life Sciences Institute and Department of Cell and Developmental Biology, University of Michigan Medical School, Ann Arbor MI 48109

ABSTRACT **Vacuolar proton-translocating ATPases (V-ATPases) are highly conserved, ATP-driven proton pumps regulated by reversible dissociation of its cytosolic, peripheral V_1 domain from the integral membrane V_o domain. Multiple stresses induce changes in V_1-V_o assembly, but the signaling mechanisms behind these changes are not understood. Here we show that certain stress-responsive changes in V-ATPase activity and assembly require the signaling lipid phosphatidylinositol 3,5-bisphosphate (PI(3,5)P_2). V-ATPase activation through V_1-V_o assembly in response to salt stress is strongly dependent on PI(3,5)P_2 synthesis. Purified V_o complexes preferentially bind to PI(3,5)P_2 on lipid arrays, suggesting direct binding between the lipid and the membrane sector of the V-ATPase. Increasing PI(3,5)P_2 levels in vivo recruits the N-terminal domain of V_o-sector subunit Vph1p from cytosol to membranes, independent of other subunits. This Vph1p domain is critical for V_1-V_o interaction, suggesting that interaction of Vph1p with PI(3,5)P_2-containing membranes stabilizes V_1-V_o assembly and thus increases V-ATPase activity. These results help explain the previously described vacuolar acidification defect in yeast *fab1Δ* and *vac14Δ* mutants and suggest that human disease phenotypes associated with PI(3,5)P_2 loss may arise from compromised V-ATPase stability and regulation.**

Monitoring Editor
John York
Vanderbilt University

Received: Oct 2, 2013
Revised: Jan 13, 2014
Accepted: Feb 5, 2014

INTRODUCTION

Vacuolar proton-translocating ATPases (V-ATPases) are highly conserved proton pumps that acidify the Golgi apparatus, endosomes, and lysosomes of all eukaryotic cells (Kane, 2006; Forgac, 2007). The yeast V-ATPase comprises 14 different subunits arranged into a peripheral complex (V_1) containing the sites of ATP hydrolysis attached to an integral membrane complex (V_o) containing the proton pore (Kane, 2006; Forgac, 2007). Modulation of V_1-V_o assembly levels is a major mechanism of V-ATPase regulation (Kane, 2006; Forgac, 2007). Glucose-responsive reversible disassembly of the V-ATPase is the best-characterized example of this type of regulation, but it has become clear that V_1-V_o assembly responds to other signals as well, including osmotic stress and elevated extracellular pH (Voss *et al.*, 2007; Diakov and Kane, 2010; Li *et al.*, 2012; Lin *et al.*, 2012). Subunits at the interface of the V_1 and V_o sectors, particularly V_1 subunit C (encoded by *VMA5*) and V_o subunit a (encoded by *VPH1* and its isoform *STV1* in yeast) are critical for V_1-V_o interactions and believed to play important roles in V-ATPase regulation by different stimuli (Kawasaki-Nishi *et al.*, 2001; Voss *et al.*, 2007; Oot and Wilkens, 2012; Rahman *et al.*, 2013). However, the signaling mechanisms governing V-ATPase assembly are not completely understood.

Phosphoinositides are a critical class of signaling molecules. They are transiently generated at specific organelles and membrane subdomains, where they can recruit effectors from the cytosol and regulate the assembly and/or activation of resident proteins (De Camilli *et al.*, 1996; Di Paolo and De Camilli, 2006; Roth, 2004; Strahl and Thorner, 2007). The inositol headgroup can be singly or multiply phosphorylated through the activity of lipid kinases, and the localized action of these kinases and the opposing phosphatases creates an organelle-specific distribution of different phosphoinositides. In

This article was published online ahead of print in MBoC in Press (http://www.molbiolcell.org/cgi/doi/10.1091/mbc.E13-10-0563) on February 12, 2014.

Address correspondence to: Patricia M. Kane (kanepm@upstate.edu).

Abbreviations used: ACMA, 9-amin-6-chloro-2-methoxyacridine; ALP, alkaline phosphatase; DIC, differential interference contrast; GFP, green fluorescent protein; MES, morpholineethanesulfonic acid; PI(3,5)P_2, phosphatidylinositol 3,5-bisphosphate; PI(4,5)P_2, phosphatidylinositol 4,5-bisphosphate; SC, synthetic complete; TAP, tandem affinity purification; TBS, Tris-buffered saline; V-ATPases, vacuolar proton-translocating ATPases; Vph1NT, N-terminal cytosolic domain of Vph1p; wt, wild type; YEPD, yeast extract/peptone/2% dextrose.

addition, the activity of lipid kinases and phosphatases is controlled by various signals and stresses, and changes in the levels of these lipids are key events in multiple signal transduction pathways (De Camilli *et al.*, 1996; Roth, 2004; Strahl and Thorner, 2007). Protein recognition of specific phosphoinositide headgroups mediates the functions of inositol phospholipids (Lemmon, 2008; Suh and Hille, 2008). Membrane proteins, and particularly transporters, are among the critical regulatory targets of these lipids. For example, plasma membrane ion channels and transporters such as the inward rectifier K^+ channel, the KCNQ K^+ channel, and a number of TRP Ca^{2+} channels require phosphatidylinositol 4,5-bisphosphate ($PI(4,5)P_2$), a phosphoinositide residing primarily in the plasma membrane, for full function and are inhibited by signaling pathways that reduce $PI(4,5)P_2$ levels (Hilgemann, 2007; Suh and Hille, 2008; Young *et al.*, 2010). In these cases, binding of the lipid headgroup to a cytosolic domain of the membrane protein leads to a conformational change that modulates activity (Suh and Hille, 2008; Young *et al.*, 2010).

Phosphatidylinositol 3,5-bisphosphate ($PI(3,5)P_2$) is a low-abundance phosphoinositide located in the endosomal and lysosomal membranes of fungi and higher eukaryotes (reviewed in Ho *et al.*, 2012; Shisheva, 2012). Phosphorylation of phosphatidylinositol 3-phosphate (PI(3)P) produces $PI(3,5)P_2$ through the action of the conserved PI 5-kinase Fab1p, also known as PIKfyve (Cooke *et al.*, 1998; Gary *et al.*, 1998). Fab1p associates with a large complex containing the scaffolding protein Vac14p and the Fig4p phosphatase, which converts $PI(3,5)P_2$ back to PI(3)P (Gary *et al.*, 2002; Botelho *et al.*, 2008; Jin *et al.*, 2008). Curiously, both Vac14p and Fig4p must be present for Fab1p function (Duex *et al.*, 2006b; Botelho *et al.*, 2008), suggesting that $PI(3,5)P_2$ levels are tightly regulated by coordinated activity of lipid kinases and phosphatases. Although basal levels of $PI(3,5)P_2$ are very low, they change dramatically and transiently in response to specific extracellular stresses (Dove *et al.*, 1997, 1999; Bonangelino *et al.*, 2002). In *Saccharomyces cerevisiae*, salt shock transiently increases $PI(3,5)P_2$ levels 20-fold above basal levels (Dove *et al.*, 1997; Duex *et al.*, 2006a). Elevated $PI(3,5)P_2$ leads to vacuolar fission, by which vacuoles increase in number and decrease in size (Cooke *et al.*, 1998; Bonangelino *et al.*, 2002; Dong *et al.*, 2010). Conversely, abolishing $PI(3,5)P_2$ production by deleting yeast *FAB1*, *VAC14*, or *FIG4* genes results in grossly enlarged vacuoles that appear to be poorly acidified (Cooke *et al.*, 1998; Gary *et al.*, 1998; Dove *et al.*, 2002; Rudge *et al.*, 2004). Loss of Vac14 or Fig4 function in mice leads to neurodegeneration and cellular vacuolation (Chow *et al.*, 2007; Zhang *et al.*, 2007; Jin *et al.*, 2008), and homozygous deletion of *FAB1* in mice is lethal (Ikonomov *et al.*, 2011; Takasuga *et al.*, 2013).

The source of the organelle acidification defect in $PI(3,5)P_2$-deficient cells is unknown. This defect and the presence of $PI(3,5)P_2$ in vacuolar and endosomal compartments rich in V-ATPases raise the tantalizing possibility that $PI(3,5)P_2$ might regulate the V-ATPase in these compartments. In this study, we test the hypothesis that V-ATPase activity and assembly are regulated by $PI(3,5)P_2$ levels and suggest that loss of organelle acidification in *fab1Δ* and *vac14Δ* mutants arises from loss of V-ATPase regulation.

RESULTS

V-ATPase disassembly in response to glucose deprivation is not controlled by $PI(3,5)P_2$

We assessed V-ATPase function in deletion mutants that lacked the Fab1p PI 5-kinase and Vac14p, a scaffold protein necessary for Fab1p function. We isolated vacuolar vesicles from wild-type, *fab1Δ*, and *vac14Δ* cells grown in rich medium and assayed V-ATPase–specific activity and proton pumping. Rapid disassembly of the V-ATPase after glucose deprivation is a major regulatory mechanism for V-ATPases, so we also compared ATPase and proton pumping activities after 20 min of glucose deprivation before cell lysis. As shown in Figure 1, V-ATPase activity in vacuolar vesicles isolated from glucose-deprived wild-type cells is ~40% lower than the activity from cells maintained in glucose, and the initial rate of proton pumping shows a comparable decrease. In *fab1Δ* and *vac14Δ* mutants, V-ATPase and proton pumping activity are significantly reduced in vacuolar vesicles isolated from both glucose-deprived and glucose-maintained cells. Of note, V-ATPase regulation in response to glucose is retained in *fab1Δ* and *vac14Δ* mutants even though V-ATPase activity in both glucose-maintained and glucose-deprived cells is significantly lower. Moreover, ATPase activity and proton pumping between the *fab1Δ* and *vac14Δ* mutants was not significantly different, even though $PI(3,5)P_2$ production is completely abolished in the *fab1Δ* strain, whereas *vac14Δ* mutants retain ~5% of the wild-type levels of this lipid (Duex *et al.*, 2006b).

We compared the protein levels of V-ATPase subunits in the isolated vacuolar vesicles by immunoblot (Figure 1C). The peripheral (V_1) sector is reversibly released from the integral membrane (V_o) sector upon glucose deprivation. Levels of the integral membrane V_o-a subunit (Vph1p) and the vacuolar marker alkaline phosphatase (ALP) are comparable in the presence and absence of glucose in all of the strains. (The appearance of the lower-mobility, unprocessed form of ALP in *fab1Δ* and *vac14Δ* is characteristic of cells with reduced V-ATPase activity because lower vacuolar protease activity reduces processing at the vacuole; Sambade *et al.*, 2005.) In contrast to the V_o subunit a, levels of V_1 subunits, particularly V_1 subunit C, decrease upon glucose deprivation (Figure 1, C and D). This reflects disassembly of V_1 from V_o at the vacuolar membrane. In *fab1Δ* and *vac14Δ* mutants, a reduction of V_1 subunits also occurs upon glucose deprivation, reflecting normal V-ATPase regulation by glucose. However, in both glucose-deprived and glucose-replete conditions, the levels of V_1 subunits in the mutants appear to be reduced relative to wild type. These results indicate that reduced V-ATPase activity and proton pumping in $PI(3,5)P_2$ mutants are at least partially accounted for by reduced assembly of V_1 subunits at the vacuolar membrane but that disassembly upon glucose deprivation is independent of $PI(3,5)P_2$ level.

V-ATPase activity and assembly increase under conditions that raise $PI(3,5)P_2$ level

$PI(3,5)P_2$ is one of the least abundant inositol phospholipids, but its level increases dramatically in response to several extracellular stresses (Bonangelino *et al.*, 2002; Duex *et al.*, 2006b; Mollapour *et al.*, 2006). The response to salt stress is best described. Addition of NaCl to the extracellular medium can induce a transient, ~20-fold increase in cellular $PI(3,5)P_2$ level (Bonangelino *et al.*, 2002; Duex *et al.*, 2006a). We previously found that V-ATPase activity and assembly can be increased by salt shock (Li *et al.*, 2012), and we tested whether this response was dependent on $PI(3,5)P_2$ by exposing *fab1Δ* cells to 500 mM NaCl for 20 min before cell lysis and vacuole isolation. As shown in Figure 2A, salt shock results in an approximately twofold increase in ATPase activity in wild-type vacuoles. In contrast, there is very little salt activation of the V-ATPase in *fab1Δ* cells. Figure 2B demonstrates that V-ATPase activation in response to salt is accompanied by increased assembly of V_1 subunits at the vacuolar membrane in wild-type cells. Of note, the increase in V_1 subunit assembly in the presence of salt is almost completely absent in the *fab1Δ* mutant. The normalized ratio of the V_1-C subunit to the V_o-a subunit (Figure 2C) parallels the changes in V-ATPase activity in response to salt. Therefore salt activation of the V-ATPase occurs, in

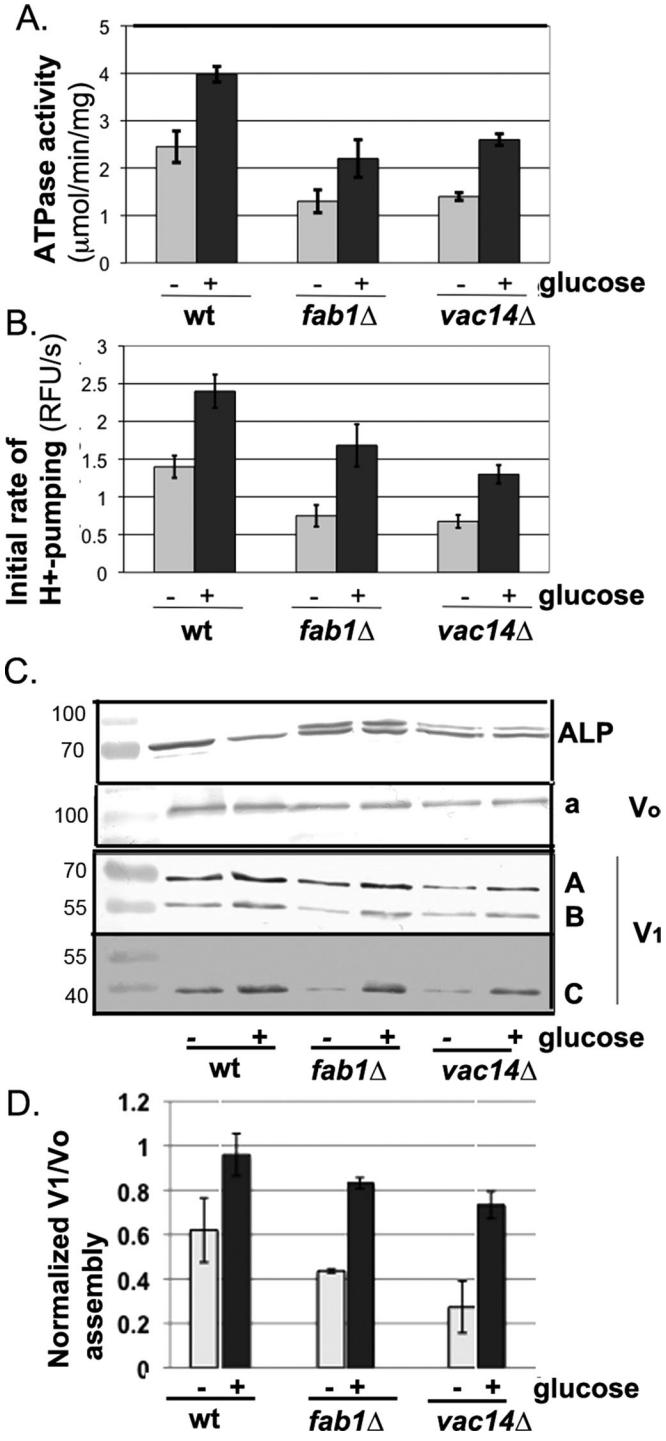

FIGURE 1: *fab1Δ* and *vac14Δ* mutants reduce ATPase activity and assembly. Vacuolar vesicles were isolated from wild-type (wt) and mutant yeast cells after growth in YEPD, pH 5, medium. (A) Concanamycin A–sensitive ATPase activity in vacuolar vesicles isolated with (+) or without (–) incubation in glucose for ~20 min just before spheroplast lysis and vacuole isolation. The mean specific activity for at least three independent vacuole preparations is shown, with error bars representing SEM. (B) The same samples described in A were tested for ATP-driven proton pumping using the ACMA quenching assay (see *Materials and Methods*). The initial rate of pumping after addition of MgATP to the vacuolar vesicles was determined, and the mean ± SEM is shown. (C) Representative immunoblot showing V-ATPase subunit levels. Vacuolar vesicles were solubilized, and the same amount of total vacuolar protein was loaded for each strain. Blots were probed with monoclonal antibodies against the indicated V-ATPase subunits or the vacuolar protein ALP. (D) Relative levels of V_1/V_o assembly in the indicated strains were quantitated by measuring the ratio of the V_1-C and V_o-a subunit signals on immunoblots of the vacuolar preparations used in A and B and then normalizing to a wild-type + glucose sample run in parallel. Mean assembly level ± SEM.

part, through increased V_1 assembly at the membrane, and this response requires $PI(3,5)P_2$ production.

We previously showed that high extracellular pH stabilizes the V-ATPase (Diakov and Kane, 2010). In cells grown at high pH, there is both increased V_1-V_o assembly and activity and less sensitivity to the glucose disassembly signal. Combining glucose deprivation with high extracellular pH yields less V_1-V_o disassembly than in normal, acidic pH. $PI(3,5)P_2$ level showed a sustained sixfold increase during high-pH stress (pH 7.6; Mollapour *et al.*, 2006), so we studied the potential role of $PI(3,5)P_2$ kinase activity in V-ATPase stabilization at high extracellular pH. Although *fab1Δ* and *vac14Δ* mutants do not exhibit the full Vma– phenotype of mutants lacking all V-ATPase activity (Sambade *et al.*, 2005), we found that both mutants grew poorly in minimal medium buffered to pH 7. The growth of the *fab1Δ* mutant was so poor that we could not obtain sufficient cells for vacuole preparation, but we were able to obtain enough *vac14Δ* cells despite its slow growth. Wild-type and *vac14Δ* cells were grown in glucose-containing minimal medium buffered to pH 5 or 7 and then exposed to media with or without glucose for 20 min before lysis. As reported previously (Diakov and Kane, 2010), wild-type vacuoles have significantly higher V-ATPase activity and less starvation-induced disassembly of the enzyme after growth in high-pH media (Figure 3A). Of interest, V-ATPase activity is also higher in vesicles isolated from the *vac14Δ* mutant grown at pH 7 compared with pH 5 (Figure 3A), but stabilization of V-ATPase during glucose deprivation is compromised. In *vac14Δ* mutants, more disassembly of V_1 sector from the vacuole membrane occurs upon glucose deprivation at high pH than in wild type (Figure 3B). Quantitation of the V_1/V_o ratio showed that there was a <15% reduction in assembly when wild-type cells grown at pH 7 were deprived of glucose. In contrast, *vac14Δ* cells showed a 48% drop in assembly with glucose deprivation at pH 7 (Figure 3C).

Taken together, these results suggest that $PI(3,5)P_2$ has a stabilizing effect on the V-ATPase. The low basal level of this lipid is necessary for full V-ATPase activity. Both activity and assembly are reduced in the *fab1Δ* and *vac14Δ* mutants, although disassembly of the enzyme in response to glucose deprivation still occurs. Increased level of $PI(3,5)P_2$ in response to extracellular salt or alkaline stress is accompanied by increased V-ATPase activity and assembly, and these changes depend on $PI(3,5)P_2$ synthesis. These data suggest an intimate connection between level of $PI(3,5)P_2$ and V-ATPase assembly but do not indicate whether this connection is direct or indirect.

Elevated $PI(3,5)P_2$ levels in a hyperactive *FAB1* mutant recruit V_1 subunits from the cytosol to the vacuolar membrane

Stabilization of V_1 assembly with V_o sectors at the vacuole by endogenous levels of $PI(3,5)P_2$ suggests that increasing $PI(3,5)P_2$ levels might help to actively recruit V-ATPase subunits to the vacuolar membrane. To test this, we expressed an extra copy of a DsRed-tagged V_1-C subunit (Vma5-DsRed) in cells containing the constitutively active *FAB1* allele, *FAB1-VLA*, as well as in wild-type cells, a *fab1Δ* mutant, and a kinase-dead *fab1-EEE* mutant. The *FAB1-VLA*

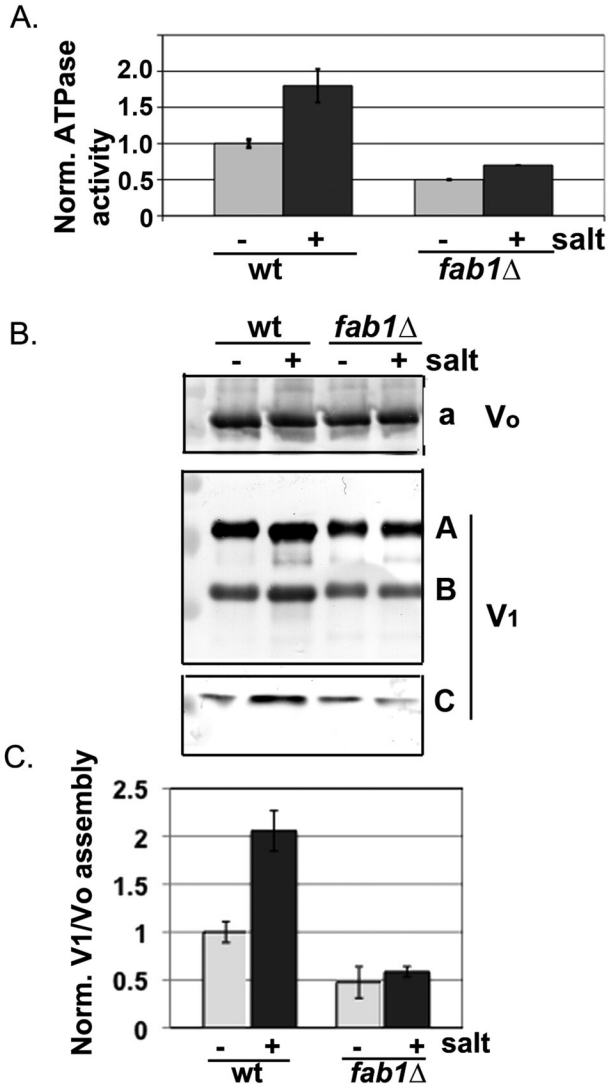

FIGURE 2: Salt activation of V-ATPase activity and assembly is $PI(3,5)P_2$ dependent. Vacuolar vesicles were prepared from wild-type and *fab1Δ* cells grown to log phase in fully supplemented minimal medium buffered to pH 5 with MES, converted to spheroplasts, and then incubated with (+) or without (–) 500 mM NaCl for 20 min before lysis. (A) Concanamycin A–sensitive ATPase activity from three independent vacuolar vesicle preparations for wt cells and two independent preparations of *fab1Δ* cells was determined and normalized to the level in wild-type cells incubated without salt. (B) Representative immunoblot showing levels of V_1 and V_o subunits. (C) Relative levels of V_1/V_o assembly determined from ratio of V_1-C and V_o-a subunit signals as described in Figure 1D and normalized to a wild-type sample without salt run in parallel.

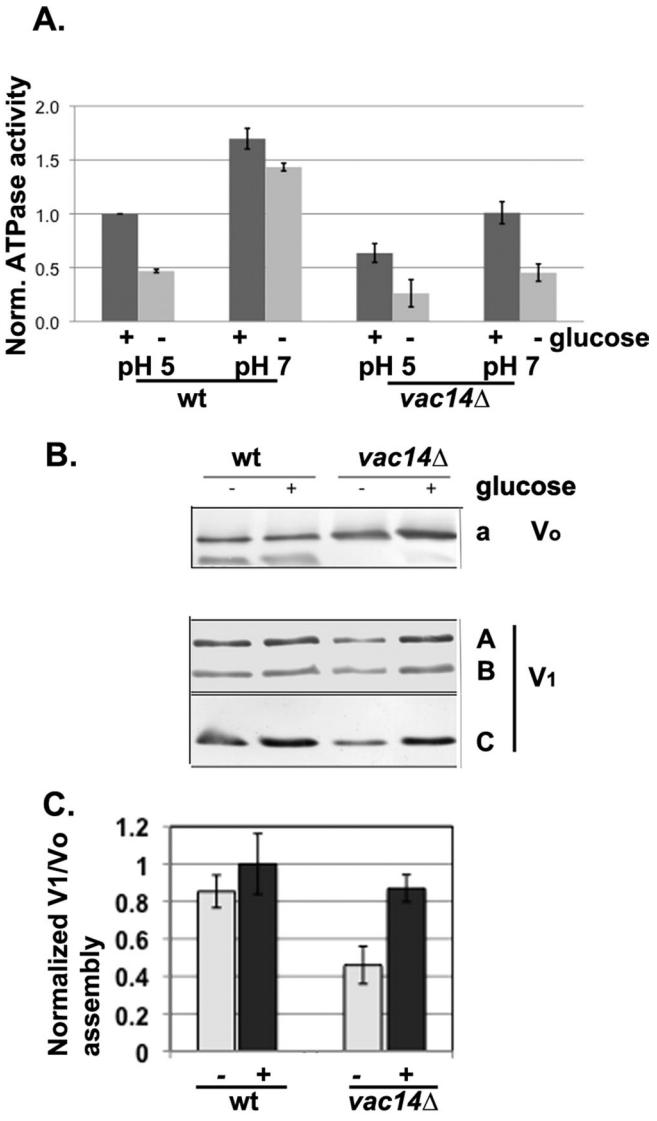

FIGURE 3: $PI(3,5)P_2$ deficiency reduces stabilization of the V-ATPase to glucose deprivation at high pH. Wild-type and *vac14Δ* cells were grown to log phase in fully supplemented minimal medium buffered to either pH 5 or 7 with 50 mM MES. Vacuolar vesicles were isolated from spheroplasts maintained in glucose (+) or deprived of glucose (–) for 20 min before lysis. (A) Mean concanamycin A–sensitive ATPase activities normalized to the activity in vesicles from wild-type cells grown at pH 5 and maintained in glucose. All are mean ± SEM for at least three independent vacuole preparations, except for the wild-type, pH 5, samples, which represent only two samples. (B) Representative immunoblot of subunit levels in vacuolar vesicles isolated from wt and *vac14Δ* mutant cells grown at pH 7 and then incubated in the presence or absence of glucose as described in Figure 1C. The lower band in the V_o-a blot is a proteolytic fragment that was observed previously but is not specific to these growth conditions. (C) Relative levels of V_1/V_o assembly determined from the ratio of V_1-C and V_o-a subunit signals as described in Figure 1D and normalized to a wild-type sample + glucose run in parallel.

mutant causes a constitutive, 17-fold increase in the cellular steady-state level of $PI(3,5)P_2$ (Duex *et al.*, 2006a). The C subunit is the only V_1 subunit that dissociates from the rest of the peripheral V_1 sector during disassembly, and reassociation of C with the V_1 sector at the vacuolar membrane is necessary for V-ATPase function (Kane, 1995; Smardon and Kane, 2007).

To visualize the vacuolar membrane and help assess of V_1-V_o assembly, we tagged the vacuolar V_o subunit Vph1p with green fluorescent protein (GFP) at its chromosomal locus (Vph1-GFP). The Vph1-GFP staining marks the vacuolar membrane; the changes in vacuolar morphology in the *fab1Δ* and *fab1* mutants seen here are comparable to those documented previously for these mutants (Duex *et al.*, 2006a). In further support of a role for Fab1p in V_1 recruitment to the membrane, we found that in the *fab1Δ* mutant, the Vma5-DsRed subunit is predominantly cytosolic and exhibits little

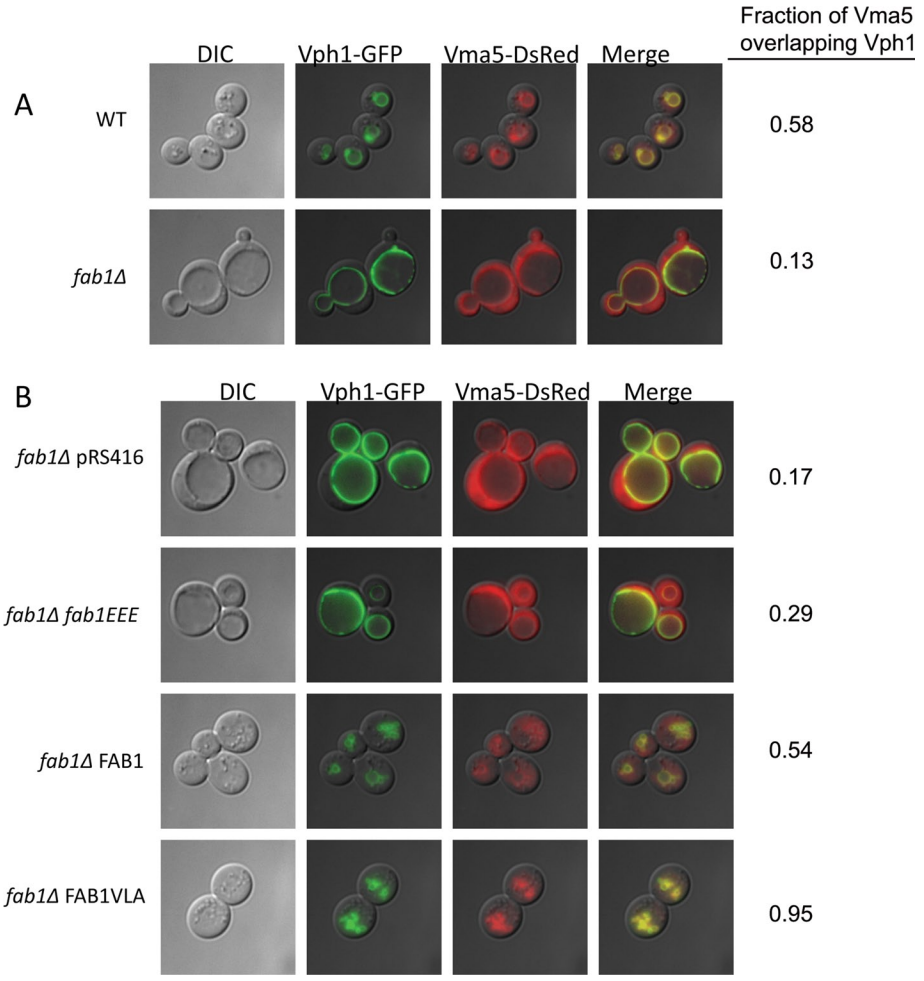

FIGURE 4: Fab1 activity promotes assembly of V_1 subunit C at the vacuole. (A) Wild-type or *fab1*Δ strains that express Vph1-GFP from its chromosomal locus were transformed with a low-copy plasmid expressing Vma5-DsRed; colocalization of the two labels indicates V-ATPase assembly. The C subunit of the V-ATPase is localized predominantly on vacuole membrane in a wild-type strain but is present at higher levels in the cytoplasm of the *fab1*Δ strain. (B) The kinase activity of Fab1 is required to promote assembly of V-ATPase. In the presence of the kinase-dead *fab1*EEE mutant or *fab1*Δ, strains in which no PI(3,5)P_2 is generated, Vma5-DsRed is mislocalized to the cytoplasm. In the dominant-active mutant Fab1VLA, PI(3,5)P_2 levels are elevated 17-fold (Duex *et al.*, 2006b). In the presence of Fab1VLA, additional Vma5-DsRed is recruited to the vacuole membrane relative to the *fab1Δ/FAB1* wild-type strain. The fraction of Vma5 overlapping Vph1 represents the Manders M1 coefficient for the fraction of the red signal (Vma5-DsRed) overlapping the green signal (Vph1-GFP), calculated as described in *Materials and Methods*.

colocalization with Vph1-GFP (Figure 4A). Note that the grossly enlarged vacuoles in the *fab1Δ* mutant are characteristic of loss of Fab1p function (Gary *et al.*, 1998). Addition of an empty plasmid (pRS416) or a kinase-dead *fab1* mutant (*fab1-EEE*) on a plasmid did not improve colocalization (Figure 4B), but wild-type *FAB1* expressed from a plasmid partially restored localization of Vma5-DsRed subunit to vacuoles, as well as restoring wild-type vacuolar morphology. Of note, a significant amount of cytosolic Vma5-DsRed subunit is still observed in the presence of the wild-type *FAB1* plasmid. Wild-type cells maintain a population of cytosolic V_1 sectors even in the presence of glucose, and low-level overexpression of *VMA5* may increase the cytosolic pool of this subunit (Keenan Curtis and Kane, 2002). However, expression of the dominant-active *FAB1-VLA* mutant resulted in complete colocalization of Vma5-DsRed subunit and Vph1-GFP, indicating that increased assembly of the tagged C subunit is possible in the presence of higher PI(3,5)P_2 level. These results indicate that more Vma5-DsRed subunit could be recruited to the vacuolar membrane when PI(3,5)P_2 level is constitutively increased.

Recruitment of Vma5-DsRed to the vacuole under conditions of elevated PI(3,5)P_2 is consistent with the increased V_1-V_o assembly shown in Figures 2 and 3, but this experiment does not distinguish direct binding of Vma5-DsRed to the membrane from recruitment as part of the V_1 complex or a partially assembled subcomplex. To determine whether recruitment of the C subunit in response to elevated PI(3,5)P_2 level depends on the presence of other V-ATPase subunits, we expressed the Vma5-DsRed construct in the context of individual V-ATPase subunit deletions in both wild-type *FAB1* and *FAB1-VLA* mutant cells. As shown in Figure 5, the Vma5-DsRed subunit is not recruited to the membrane in the *FAB1-VLA* mutant when other V_1 subunits (*vma2Δ*, *vma8Δ*, *vma10Δ*, and *vma13Δ*) or V_o subunit c (*vma3Δ*) are missing. These results show that the Vma5-DsRed subunit is not recruited directly to PI(3,5)P_2 in the *FAB1-VLA* mutant but instead binds as part of the V-ATPase complex, requiring both intact V_1 and V_o subcomplexes.

Purified yeast V_o sectors show preferential binding to PI(3,5)P_2

Membrane recruitment of V_1 subunit C in response to elevated PI(3,5)P_2 requires the integral membrane V_o subcomplex, and portions of this subcomplex are in close proximity to phospholipid headgroups (Benlekbir *et al.*, 2012; Oot and Wilkens, 2012). This supports a model in which the effects of PI(3,5)P_2 on V-ATPase assembly are mediated through lipid interactions in the V_o complex. To address this, we first tested for direct binding of PI(3,5)P_2 to the V_o complex in vitro. Assembled V_o complexes were isolated from a solubilized membrane fraction of a *vma2Δ* mutant strain (which fails to assemble V_1 but contains assembled V_o sectors in the vacuolar membrane; Doherty and Kane, 1993) via a tandem affinity purification (TAP) tag on the C-terminus of Vph1p. As shown in Figure 6A, the isolated complexes contain the five bands characteristic of the six-subunit yeast V_o complex (the c and c′ subunits run together). Solubilized and purified V_o complexes were concentrated by filtration and then diluted and incubated with a "PIP blot" to probe for phosphoinositide-specific binding. Binding was detected with an anti-Vph1–specific monoclonal antibody. As shown in Figure 6B, preferential binding to PI(3,5)P_2 and PI(4)P was detected. Selective recognition of PI(3,5)P_2 over PI(3,4)P_2, PI(4,5)P_2, and PI(3,4,5)P_3 was observed repeatedly with independent V_o preparations. Recognition of the monophosphate lipids was more variable. These results suggest that the effects of PI(3,5)P_2 on the V-ATPase may be mediated by direct binding of the

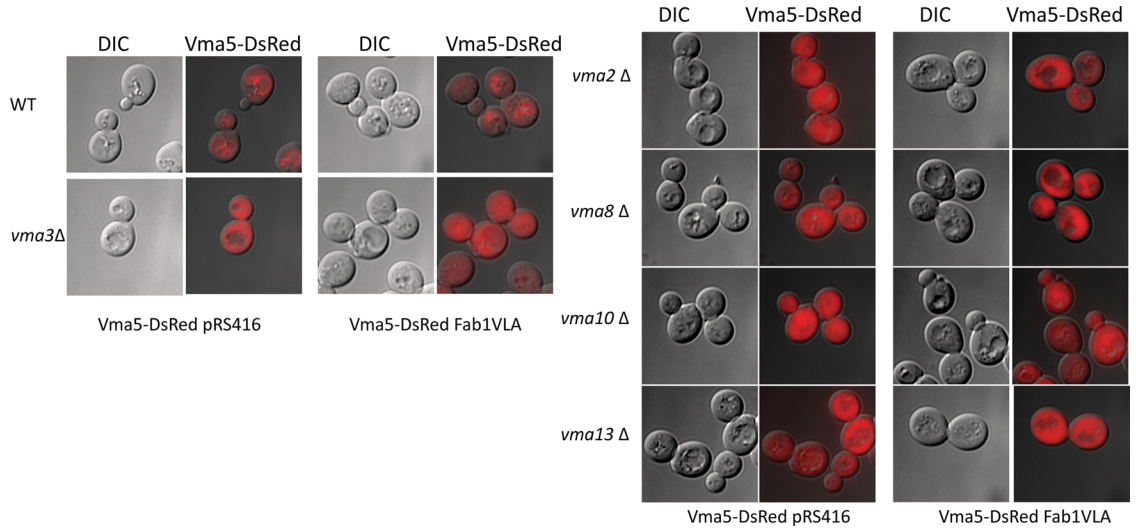

FIGURE 5: V_1 subunits and V_o subunit Vma3p are required for the vacuole membrane localization of Vma5-DsRed. Vma5DsRed was expressed from a low-copy plasmid in wild type, a mutant that disrupts V_o assembly (*vma3Δ*), and several strains that disrupt V_1 subunits (*vma2Δ*, *vma8Δ*, *vma10Δ*, and *vma13Δ*). The mutant strains were also transformed with a pRS416 plasmid control or pRS416 containing Fab1VLA to examine the effects of $PI(3,5)P_2$ overproduction in the mutants. Vacuolar localization of Vma5-DsRed is indicated by colocalization with the rim of the vacuolar membrane visualized under DIC.

lipid to the membrane-bound V_o sector. However, association with PIP blots is an in vitro method to assess physical interactions with lipid species that has a number of limitations, and so we conducted further in vivo assays to look at membrane binding of integral V_o-sector subunits in conditions that change $PI(3,5)P_2$ levels.

The Vph1NT domain is recruited to intracellular membranes under conditions that increase $PI(3,5)P_2$ levels

Vph1p contains a large cytosolic N-terminal domain (Vph1NT) along with a C-terminal domain containing multiple transmembrane helices. Structural information places the N-terminal region of Vph1p at the interface of the V_1 and V_o sectors in the holoenzyme, where it is a potential site for enzyme regulation (Diepholz *et al.*, 2008; Zhang *et al.*, 2008b; Muench *et al.*, 2009; Benlekbir *et al.*, 2012; Oot and Wilkens, 2012; Rahman *et al.*, 2013). This domain also establishes stabilizing interactions between the V_1 and V_o sectors, congruent with a role in controlling V_1-V_o stability and V-ATPase function (Oot and Wilkens, 2010; Rahman *et al.*, 2013). We created a fluorescently tagged version of Vph1NT by replacing the C-terminal region of Vph1p, including the transmembrane helices, with GFP. This construct does not complement the phenotype of a *VPH1* deletion, and both V_1 and V_o subunits are absent from the vacuolar membrane when this construct is expressed (Manolson *et al.*, 1992). However, if a binding site for $PI(3,5)P_2$ exists in the Vph1NT domain, then the tagged construct might be recruited to membranes that have increased $PI(3,5)P_2$ concentration in the absence of the other subunits.

We assessed recruitment of the Vph1NT-GFP construct to intracellular membranes by microscopy. We used two strategies to increase cellular $PI(3,5)P_2$ level. In the first approach, we exposed cells to salt shock (0.5 M NaCl) and monitored changes in Vph1NT-GFP localization over time. Previous work suggests that salt shock induces a rapid, transient increase in cellular level of $PI(3,5)P_2$ (Duex *et al.*, 2006a). Vph1NT-GFP diffusely stains the cytosol of cells grown in low-salt media. On salt exposure, it is transiently recruited to intracellular compartments (Figure 7A). Localization to membranes is first observed ~2 min after salt shock, peaks at 6–7 min of salt exposure, and then is lost by 16 min. This recruitment depends on $PI(3,5)P_2$—it does not occur in a *vac14Δ* mutant (Figure 7A). A time course of Vph1NT-GFP recruitment in a single salt-treated cell is shown in Supplemental Figure S1.

In the second approach, we increased $PI(3,5)P_2$ level with the constitutively active *FAB1-VLA* mutant described earlier. Consistent with Figure 7A, cells containing Vph1NT-GFP and only the wild-type *FAB1* allele show little colocalization of the GFP signal with the

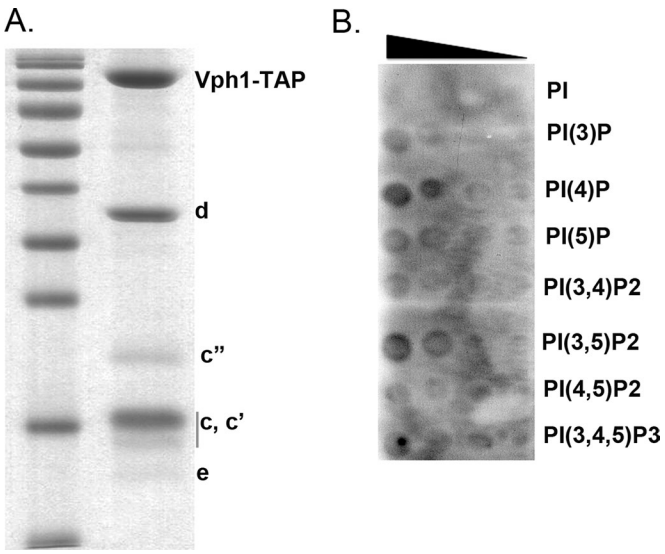

FIGURE 6: Isolated V_o sectors contain a binding site for $PI(3,5)P_2$. (A) Purified V_o sectors were separated by SDS–PAGE and then visualized by Coomassie blue staining. V_o subunits (right lane) are identified by molecular mass relative to molecular mass markers (from bottom: 10, 17, 26, 34, 43, 55, 72, 95, 130, 170 kDa). (B) PIP blot (Echelon) probed with purified V_o subunits at 80 µg/ml final concentration and binding detected with a monoclonal antibody to Vph1p. Immobilized lipids are identified to the right of the blot; the blot contains a serial dilution of the lipids going from left to right.

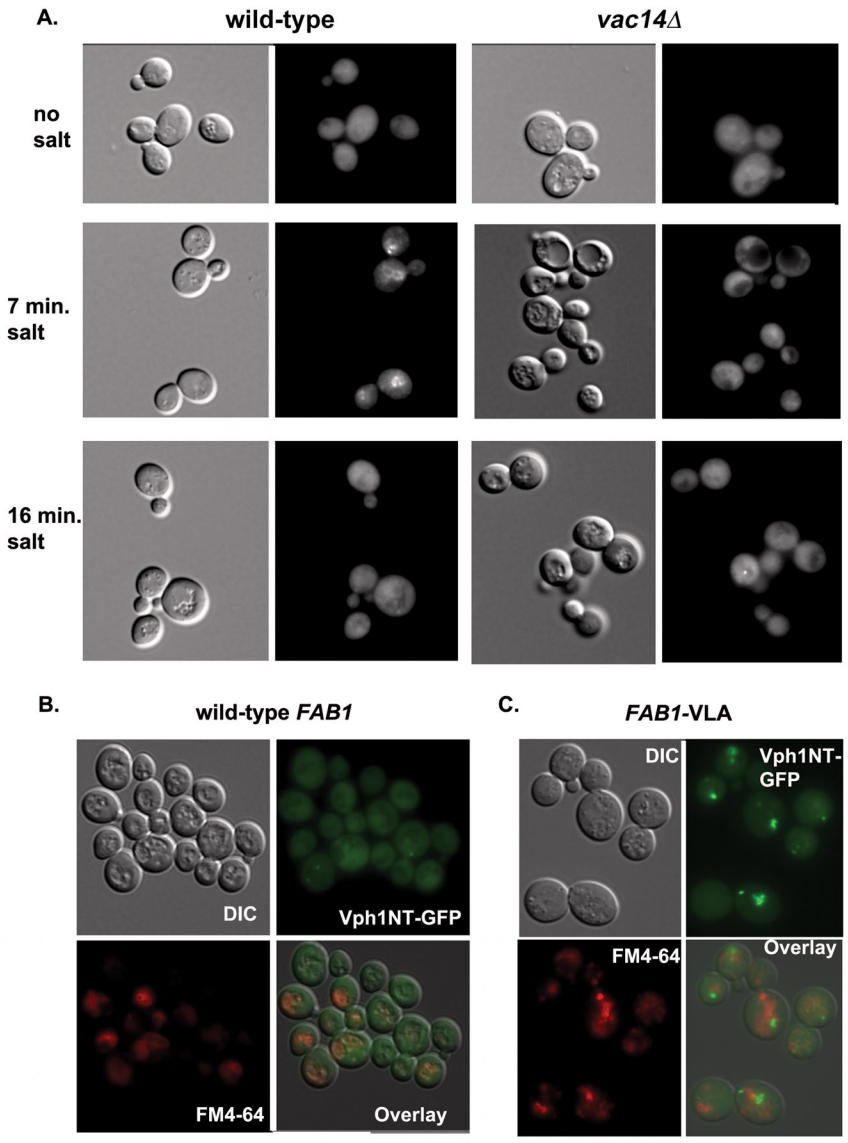

FIGURE 7: Elevation of PI(3,5)P_2 levels results in recruitment of Vph1NT-GFP to membranes. (A) Vph1NT-GFP was integrated at the *VPH1* locus in a wild-type or *vac14Δ* background as described in *Materials and Methods*. Log-phase cells were visualized directly (no salt) or at 7 and 16 min after addition of NaCl to a final concentration of 500 mM. For each set of conditions, a DIC image is shown on the left and GFP fluorescence on the right. Vph1NT-GFP recruits reversibly to membranes in the wild-type but not the *vac14Δ* cells. (B) Cells containing Vph1NT-GFP and only a wild-type FAB1 allele were labeled with the vacuolar membrane marker FM4-64. Individual DIC, GFP, and Texas red (FM4-64) images are combined in the overlay. (C) Cells containing Vph1NT-GFP were transformed with the constitutively active *FAB1-VLA* allele and labeled with the vacuolar membrane marker FM4-64. Individual DIC, GFP, and Texas red (FM4-64) images are combined in the overlay. Vph1NT-GFP and FM4-64 staining are adjacent but generally not overlapping.

vacuole-specific FM4-64 label in Figure 7B. However, like salt shock, expression of the *FAB1-VLA* allele led to the localization of Vph1NT-GFP to puncta (Figure 7C), indicating that higher PI(3,5)P_2 production leads to relocalization of Vph1NT to intracellular membranes. However, vacuolar-specific FM4-64 staining consistently showed recruitment of Vph1NT-GFP to structures distinct from, but adjacent to, vacuoles (Figure 7C, overlay). The fraction of the Vph1NT-GFP signal overlapping the FM4-64 signal in Figure 7, B and C, was quantitated as described in *Materials and Methods*. The Manders M2 coefficient, which describes the fractional overlap, was 0.16 for *FAB1* wild-type cells and 0.14 for *FAB1*-VLA cells. This indicates that there was very little overlap of the signals, despite the extensive recruitment of Vph1NT-GFP to membranes in the *FAB1*-VLA samples. Salt treatment of cells after staining with FM4-64 also indicated that recruited Vph1NT-GFP localized adjacent to FM4-64–stained vacuoles (unpublished data). This staining pattern may be consistent with recruitment of Vph1NT-GFP to late endosomes, perivacuolar membranes that also contain PI(3,5)P_2, rather than vacuoles.

The phenotypes described in Figures 1–3 indicate stabilization of the V-ATPase in vacuolar membranes, but the Vph1NT-GFP construct did not appear to reach the vacuolar membrane. It is possible that Vph1NT-GFP is initially recruited to late endosomes because they contain the highest PI(3,5)P_2 levels, but that this interaction cannot be sustained in the absence of other interactions available to the intact enzyme. Several PI(3)P-binding FYVE domains support binding to PI(3)P in the context of intact proteins but cannot localize to PI(3)P-containing membranes as isolated as FYVE-GFP fusions (Hayakawa *et al.*, 2004). Dimerization of these FYVE domains can increase avidity for the membrane and allow PI(3)P-dependent recruitment. To address this possibility, we constructed a Vph1NTNT-GFP containing a tandem fusion of two Vph1NT domains followed by GFP. The Vph1NTNT-GFP protein is also largely cytosolic when cells are grown in low-salt medium but is recruited to FM4-64–stained vacuoles in response to salt (Figure 8). Recruitment to membranes is sustained for longer periods than recruitment of the single Vph1NT-GFP, as shown by the extensive recruitment after 14 min of salt exposure. These results provide in vivo evidence that Vph1NT is able to independently bind to vacuoles under conditions that increase PI(3,5)P_2, suggesting that there is a binding site for the lipid on this subunit.

DISCUSSION

V-ATPase assembly and stability can be regulated by PI(3,5)P_2 level

V-ATPase assembly and activity are responsive to multiple extracellular stimuli (Kane, 1995; Diakov and Kane, 2010; Batelli *et al.*, 2007; Li *et al.*, 2012), but the signaling pathways responsible for this response have remained elusive. These results highlight one signaling pathway that regulates V-ATPase assembly and activity. Remarkably, the V-ATPase both requires the very low basal level of PI(3,5)P_2 present during growth for full activity (Figure 1) and responds to changes in PI(3,5)P_2 levels in the presence of specific extracellular stresses (Figures 2 and 3). V-ATPase activation in response to hyperosmotic stress is highly dependent on PI(3,5)P_2 synthesis, and stabilization of the V-ATPase at high extracellular pH appears to

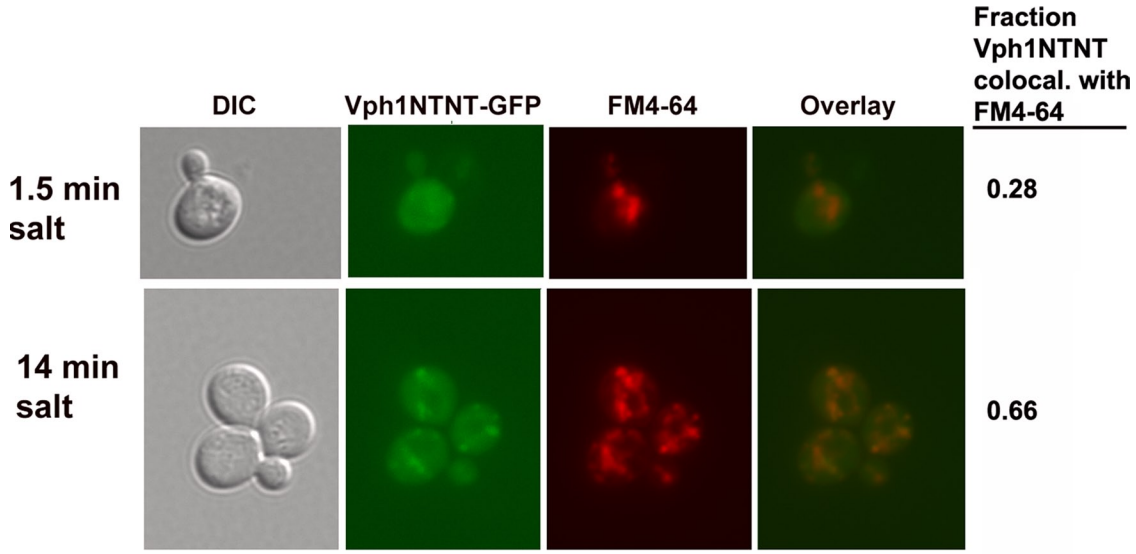

FIGURE 8: Vph1NTNT-GFP is recruited to the vacuolar membrane in response to salt. Cells containing a tandem duplication of Vph1NT attached to GFP (Vph1NTNT-GFP) labeled with FM4-64 were visualized 1.5 and 14 min after addition of 500 mM NaCl. Images viewed under DIC, GFP, and Texas red (FM4-64) filter sets are shown, together with an overlay of the GFP and Texas red channels. The fraction of Vph1NTNT colocalizing with FM4-64 represents the Manders M2 coefficient for the fraction of the green signal (Vph1NTNT-GFP) overlapping the red signal (FM4-64), calculated as described in *Materials and Methods*. There is increased overlap in the Vph1NTNT-GFP and FM4-64 staining after 14 min of salt treatment.

have both PI(3,5)P_2-dependent and -independent components. In contrast, loss of PI(3,5)P_2 has little effect on reversible disassembly of the V-ATPase in response to glucose (Figure 1D). This suggests that a distinct glucose-responsive signaling pathway continues to operate in PI(3,5)P_2-deficient mutants. Taken together, the results indicate that PI(3,5)P_2 is a significant regulator of V-ATPase assembly and activity, although not the exclusive regulator.

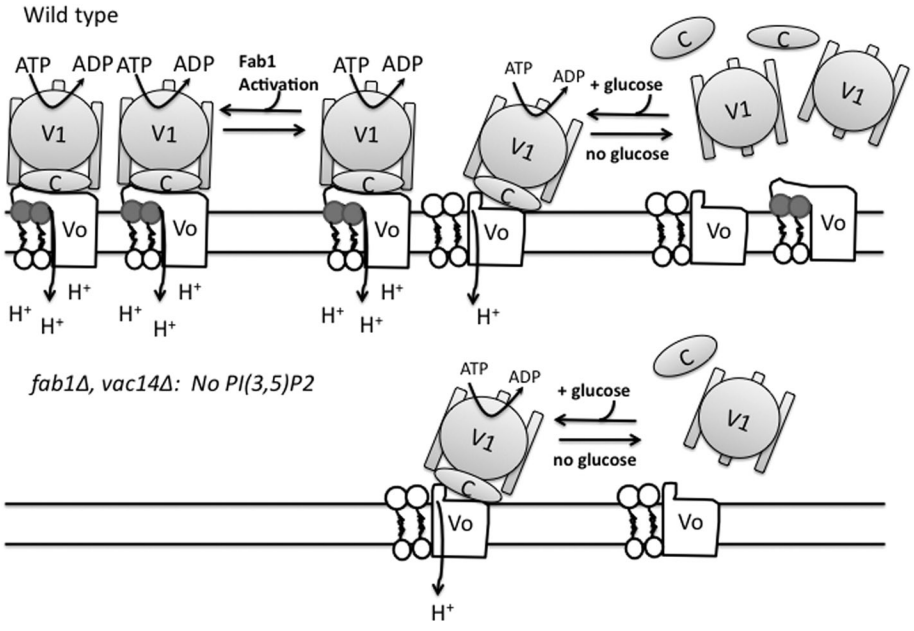

FIGURE 9: Model for stabilization of V_1-V_o interactions by PI(3,5)P_2. A conformational change in the V_o sectors, arising from binding of the Vph1NT domain to the PI(3,5)P_2 headgroup (shown in dark gray), is portrayed as giving stronger V_1-V_o binding and higher ATPase activity and H^+-transport. Complete loss of PI(3,5)P_2 in the *fab1Δ* mutant precludes access to this conformation, resulting in lower ATPase activity and lower levels of assembly. Wild-type cells in which PI(3,5)P_2 synthesis has not been activated will have both PI(3,5)P_2-bound and unbound fractions. Both PI(3,5)P_2-bound and unbound V-ATPases are susceptible to disassembly in response to glucose deprivation; this suggests that glucose signaling does not occur through PI(3,5)P_2.

How could PI(3,5)P_2 regulate V-ATPase activity?

We provide evidence that PI(3,5)P_2 binds in the membrane V_o sector of the V-ATPase—specifically, the cytosolic N-terminal domain of the largest membrane subunit, Vph1NT. Vph1NT occupies a key position at the interface of the V_1 and V_o sectors in the V-ATPase and provides critical contacts to several subunits of the peripheral V_1 sector (Benlekbir *et al.*, 2012; Oot and Wilkens, 2012). It is thus positioned to stabilize the overall V_1-V_o interaction, and in fact, has been implicated in regulating V_1-V_o assembly (Kawasaki-Nishi *et al.*, 2001). An emerging body of work reveals that the activity of many transmembrane channels and transporters is modulated by phosphoinositides. In this context, lipids often induce conformational changes by binding to a cytosolically exposed domain (Hilgemann, 2007; Suh and Hille, 2008). V-ATPase activation by PI(3,5)P_2 could occur by a similar mechanism as depicted in Figure 9. In this mechanism, the binding of Vph1NT to PI(3,5)P_2 would induce a V_o conformation that binds more stably to the V_1 sector, recruiting higher levels of V_1 to the membrane at steady state and thus increasing V-ATPase activity. Consistent with such a model, Vph1NT undergoes a significant conformational change when it is

not bound to V_1 (Wilkens and Forgac, 2001; Qi and Forgac, 2008). This change is believed to silence proton translocation and block V_1 interaction and might be susceptible to modulation by lipid interactions. Excess V_1 and V_o sectors that are not assembled into active complexes are present even in wild-type cells (Kane, 1995; Parra *et al.*, 2000) and could provide a pool of V_o sectors susceptible to PI(3,5)P_2 intervention. The absence of a PI(3,5)P_2-stabilized V_o conformation in a *fab1Δ* or *vac14Δ* mutant reduces assembly of V_1 subunits at the membrane with no reduction in the total cellular levels of V_1 subunits, suggesting a shift toward disassembled V_1 and V_o complexes. In contrast, increasing PI(3,5)P_2 levels, through hyperosmotic stress, would increase the population of Vph1NT in the stabilizing conformation, resulting in higher levels of V_1 binding and activity.

We do not yet know the binding motif in Vph1NT responsible for PI(3,5)P_2 interaction. Specific lipid-binding peptide motifs for PI(4,5)P_2 and PI(3)P have been determined, but it is also clear that a number of lipid-binding sites are three dimensional and require protein folding (Lemmon, 2008; Baskaran *et al.*, 2012). A limited number of PI(3,5)P_2-binding proteins are known, and there are no well-defined binding motifs. In addition, there is no high-resolution structure of yeast Vph1NT, but the related yeast Stv1NT isoform has been modeled based on the structure of an archaeal homologue (Srinivasan *et al.*, 2011; Finnigan *et al.*, 2012), allowing comparison to known PI(3,5)P_2-binding proteins. Several PROPPIN proteins have been shown to bind PI(3,5)P_2 (Baskaran *et al.*, 2012; Tamura *et al.*, 2013), but the β-propellers involved in binding by these proteins are not present in Vph1NT. The N-terminal 70 amino acids of the intracellular Ca^{2+}-release channel TRPML1 contain a PI(3,5)P_2-binding site that controls channel opening but has detectable homology to neither Vph1NT nor PROPPIN-like sequences. Also note that although the Vph1NTNT-GFP showed better vacuolar recruitment than Vph1NT, there is little evidence that Vph1NT is dimerized in the intact enzyme. In the intact V-ATPase, Vph1NT is anchored in proximity to the membrane by the rest of the complex, and this could easily provide the increased avidity required to bind Vph1NT to PI(3,5)P_2 in the vacuolar membrane.

Potential implications of the V-ATPase as a PI(3,5)P_2 target

Localized signaling has been proposed as one of the main advantages of phosphoinositides as signaling molecules (Suh and Hille, 2005, 2008) and could reinforce other V-ATPase regulatory mechanisms, such as isoform composition (Forgac, 2007). In plants, activation of V-ATPase activity in response to salt stress has been proposed to drive organellar salt sequestration by providing a pH gradient to drive Na^+/H^+ exchangers (Queiros *et al.*, 2009; Silva and Geros, 2009). Because these exchangers reside in endosomes and lysosomes, where PI(3,5)P_2 is enriched, activation via PI(3,5)P_2 would localize V-ATPase activation to sites of salt uptake.

Vacuolar acidification defects, based on defective uptake of the lysosomotropic amine quinacrine, have been documented in yeast mutants compromised in PI(3,5)P_2 biosynthesis (Cooke *et al.*, 1998; Gary *et al.*, 1998; Dove *et al.*, 2002; Rudge *et al.*, 2004). Reduced V-ATPase activity is likely to be directly responsible for these defects. Compromised V-ATPase function and organelle acidification defects could also account for certain PI(3,5)P_2-associated phenotypes in other systems. Fibroblasts and neurons cultured from mouse mutants deficient in PI(3,5)P_2 synthesis exhibit defects in membrane-trafficking pathways such as endosome-to–*trans*-Golgi network retrograde trafficking (Chow *et al.*, 2007; Zhang *et al.*, 2007). Similar phenotypes can also be seen in cultured mammalian cells that overexpress dominant-negative *FAB1* (Ikonomov *et al.*, 2003), as well as in cells from *Caenorhabditis elegans* and *Drosophila* with *FAB1*/PIKfyve mutations (Nicot *et al.*, 2006; Rusten *et al.*, 2006). V-ATPase activity is very important in endolysosomal trafficking and thus may well contribute to these phenotypes (Yan *et al.*, 2009). The neurological disease Charcot–Marie–Tooth 4J maps to mutations in the human Fig4 gene (Chow *et al.*, 2007), and distinct mutations in Fig4 have been linked to amyotrophic lateral sclerosis and primary lateral sclerosis (Chow *et al.*, 2009). Mice lacking Vac14 or Fig4 function also exhibit profound neurodegeneration and cellular vacuolation (Chow *et al.*, 2007; Zhang *et al.*, 2007; Jin *et al.*, 2008). In each of these cases, the underlying causes of the neurological defects have not yet been fully determined. Both defective trafficking and defective autophagy have been cited as possible roots of the degeneration (Chow *et al.*, 2007; Zhang *et al.*, 2008a; Ferguson *et al.*, 2009). The V-ATPase plays a central role in autophagy as well as trafficking pathways (Forgac, 2007; Walls *et al.*, 2010). Thus, compromised V-ATPase function may well contribute to disease phenotypes associated with loss of PI(3,5)P_2 homeostasis.

MATERIALS AND METHODS

Media

Yeast extract/peptone/2% dextrose (YEPD) medium was buffered to pH 5.0 with 50 mM potassium phosphate and 50 mM potassium succinate as described (Yamashiro *et al.*, 1990). Synthetic complete (SC) medium was prepared as in Amberg *et al.* (2005) and buffered to pH 5 or 7 with 50 mM morpholineethanesulfonic acid (MES) as described (Diakov and Kane, 2010). For vacuolar vesicle preparations, yeast were grown to log phase in either in YEPD, pH 5.0, or buffered SC media as described (Diakov and Kane, 2010).

Yeast strains and plasmids

Yeast *fab1Δ*, and *vac14Δ* mutants in the BY4741 strain background were purchased as part of a yeast deletion mutant array from Open Biosystems (Pittsburgh, PA). The *fab1Δ::kanMX* and *vac14Δ::kanMX* alleles were PCR amplified from the mutant strains with oligonucleotides flanking the deletion and then transformed into wild-type yeast strain SF838-5Aα (*MAT* α *leu3-2, 112, ura3-52, ade6, gal2).* All vacuolar vesicle preparations were from the SF838-5Aα strain background.

Purification of vacuoles and biochemical analysis

Cells were grown to log phase, converted to spheroplasts, and lysed, and vacuolar vesicles were isolated by Ficoll density gradient centrifugation (Roberts *et al.*, 1991). ATP hydrolysis rates were determined on freshly prepared vacuolar vesicles by a coupled enzyme assay described previously (Liu *et al.*, 2005); concanamycin A was added directly to the assay mixture to a final concentration of 100 nM to determine inhibitor-sensitive activity. Specific V-ATPase activity represents the rate of concanamycin A–sensitive ATPase hydrolysis, expressed as micromoles of ATP consumed/minute per milligram of vacuolar protein. Proton pumping was observed using the 9-amino-6-chloro-2-methoxyacridine (ACMA) quenching assay described previously (Liu *et al.*, 2005). A 10-μg amount of vacuolar vesicles was used for each assay. Pumping was initiated by adding 0.5 mM ATP and 1.0 mM $MgSO_4$. The rate of proton pumping is represented by the initial rate (first 15 s after MgATP addition) of ACMA fluorescence quenching in the presence or absence of 100 nM concanamycin A and is normalized to the amount of vacuolar protein added.

For determination of salt-responsive of V-ATPase activity, wild-type and mutant cells were converted to spheroplasts, resuspended in synthetic complete medium containing 1.2 M sorbitol with or

without 500 mM NaCl, and incubated at 30°C for 20 min before cell lysis and isolation of vesicles (Li *et al.*, 2012). For examination of extracellular pH dependence of V-ATPase activity, wild-type and *vac14Δ* mutant cells were grown in synthetic complete medium buffered to pH 5 or 7 with 50 mM MES and then incubated with or without glucose addition after spheroplasting as described (Diakov and Kane, 2010).

For Western blot analysis, vacuolar vesicles were solubilized in cracking buffer, separated by SDS–PAGE, and transferred to nitrocellulose as described (Smardon and Kane, 2007). V-ATPase subunits were detected with mouse monoclonal antibodies 10D7 (anti-Vph1p), 8B1 (anti–V_1-A subunit), 13D11 (anti–V_1-B subunit), and 7A2 (anti–V_1-C subunit; Kane *et al.*, 1992). The vacuolar marker ALP was detected with monoclonal antibody 1D3A10 (Life Technologies, Grand Island, NY). Quantitation was done using ImageJ 1.48g (National Institutes of Health, Bethesda, MD). For each independent vacuole preparation, signals from the V_1-C and V_o-a immunoblots were quantitated (for loads determined to be in the linear range of detection), and the ratio of the two signals, representative of the level of V_1/V_o assembly, was normalized to the ratio of a wild-type sample run in parallel. The variation in ratios for wild-type samples was determined by comparing multiple wild-type samples on the same immunoblot.

Colocalization of DsRed-tagged Vma5p with Vph1-GFP

In both fab1Δ and wild-type (LWY7235 *MATa*, *ura3-52*, *leu2-3,-112*, *his3-Δ200*, *trp1-Δ901*, *lys2-801*, *suc2-Δ9*) yeast, *VPH1* fused with green fluorescent protein at its C-terminus was integrated into the *VPH1* locus and expressed from its endogenous promoter. The integrated allele was generated using the GFPKanMX6 cassette and standard protocols. To generate pRS-416-*VMA5*-DsRed, PCR was used to amplify the open reading frame of *VMA5* without the stop codon, along with 1 kb of upstream genomic DNA, and introduced into pDONR221 by recombination-based cloning (Gateway system; Invitrogen, Grand Island, NY). The *VMA5* entry clone was introduced into the pAG416-ccdB-DsRED destination vector (Addgene, Cambridge, MA).

For colocalization studies, overnight cultures were diluted to 5×10^6 cells/ml in SC-Ura medium. After two additional doublings, cells were visualized with fluorescence and differential interference contrast (DIC) microscopy. Images were generated with a DeltaVision system (Applied Precision, Issaquah, WA).

Isolation of V_o sectors and analysis of binding to PIP arrays

V_o complexes were kindly provided by Sergio Couoh-Cardel and Stephan Wilkens (SUNY Upstate Medical University, Syracuse, NY). The V_o complexes were purified from a membrane fraction solubilized in dodecyl maltoside and then isolated via a TAP tag on *VPH1* from a *vma2Δ* strain containing *VPH1*-TAP (S. Couoh-Cardel and S. Wilkens, unpublished data). The purified V_o was provided at 26 mg/ml protein and then diluted in blocking buffer (20 mM Tris, pH 7.5, 500 mM NaCl, 3% fatty acid–free bovine serum albumin [BSA]) containing 0.02% dodecyl maltoside (Anatrace, Santa Clara, CA) to 80 μg/ml before probing the PIP Arrays (Echelon Research Laboratories, Salt Lake City, UT), which were blocked with blocking buffer for 1 h. All blocking, incubation, and wash steps were done with shaking at room temperature. Purified V_o sectors were incubated with the PIP Array at a final concentration of 80 μg/ml for 1 h. After this incubation, membranes were washed three times in Tris-buffered saline (TBS; blocking buffer without BSA) for 10 min each, incubated with anti–V_o-a subunit antibody (10D7; Kane *et al.*, 1992) in blocking buffer for 1 h, washed another three times in TBS, and incubated with horseradish peroxidase–conjugated anti-mouse immunoglobulin G in blocking buffer for 1 h (Bio-Rad, Hercules, CA). After three washes in TBS, membranes were developed by enhanced chemiluminescence Western blotting detection reagent (GE Healthcare, Piscataway, NJ) and exposed to film for 1–3 s.

Construction and imaging of Vph1NT-GFP and Vph1NTNT-GFP

Vph1NT-GFP was constructed by genomic integration of GFP and a kanMX marker immediately after the sequence for amino acid 406 of Vph1p. The pFA6-GFPKanMX plasmid (Longtine *et al.*, 1998) was used as a template for PCR amplification using oligonucleotides 5′*TTCCAAAGTATCTGTGACTGTTACGGTATTGCTCAGTACAGA-GAAATCAAT*CGGATCCCCGGGTTAATTAA3′ and 5′*GCTTGAA-GCGGAAGAGCTTGCACTAGCAACAGCGACTTCCATGTCTTTATA*-GAATTCGAGCTCGTTTAAAC3′, in which 51 bases of *VPH1* sequence upstream and downstream of the insertion are italicized. The PCR product was then transformed into SF838-5Aα (wild type) or the congenic *vac14Δ* mutant cells, and transformants were selected by growth on YEPD containing μg/ml G418. Transformants were then screened for production of the ~75-kDa Vph1NT-GFP fusion protein by immunoblot. The construct removes the C-terminal transmembrane helices of Vph1p and replaces them with GFP. To construct the Vph1NTNT-GFP strain containing a tandem duplication of the first 406 amino acids of *VPH1*, genomic DNA was prepared from cells containing the Vph1NT-GFP-kanMX construct and used as a template for PCR amplification using oligonucleotides 5′*TTCCAAAGTATCT-GTGACTATTACGGTATTGCTCAGTACAGAGAAATCAAT*ATGGCA-GAGAAGGAGGAAGC3′ (italicized nucleotides correspond to the sequence at the end of VPH1NT, and the final 20 nucleotides correspond to the beginning of *VPH1* open reading frame) and 5′AACGTTTTCATGAGATAAGTTTGGC3′ (complementary to a sequence 200 base pairs downstream from the *VPH1* open reading frame). The 4-kb PCR product was isolated and transformed into SF838-5Aα cells, and transformants were selected by growth on G418 plates.

To increase $PI(3,5)P_2$ levels by salt treatment, cells were resuspended in SC medium and NaCl added to a final concentration of 500 mM at time 0. The cells were then transferred to a slide and visualized over time. FM4-64 was purchased from Invitrogen. Vph1NT-GFP cells grown to log phase were suspended in YEPD, pH 5, at a density of 1 OD unit/ml and incubated with 8 μM FM4-64 for 60 min at 30°C. The cells were then pelleted by centrifugation, washed once in YEPD, pH 5, resuspended at the same density in YEPD, pH 5, and incubated for a 75-min chase period at 30°C. After the chase, cells were washed and resuspended in SC medium before visualization by fluorescence microscopy. GFP-tagged proteins and FM4-64 labeling were visualized on a Zeiss Imager Z1 fluorescence microscope using GFP and Texas red filter sets, respectively. Fluorescent and DIC images were captured with a Hamamatsu charge-coupled device camera and analyzed with AxioVision 4.8 software (Carl Zeiss Company, Peabody, MA). Figures were prepared using Photoshop 11.0.4 (Adobe, San Jose, CA).

Quantitation of overlap from micrographs

The extent of colocalization was quantitated using the Just Another Colocalization Plug-in (Bolte and Cordelieres, 2006) in ImageJ 1.48g. The same fields of cells labeled with GFP-tagged protein and either DsRed-labeled protein (Figure 4) or FM4-64 (Figures 7 and 8) were submitted, and the Manders coefficients M1 (fraction of red signal overlapping green) and M2 (fraction of green signal overlapping red) were calculated. Threshold values

were generated by the plug-in. The M1 and M2 coefficients with automatic threshold were used in Figures 4 and 7. For Figure 8, the M2 coefficient with Costes' threshold was used because lower expression of the Vph1NTNT-GFP construct results in a low GFP signal relative to the FM4-64 signal (Bolte and Cordelieres, 2006).

ACKNOWLEDGMENTS

This work was supported by National Institutes of Health Grants R01 GM50322 to P.M.K. and R01-GM050403 to L.S.W. We thank Stephan Wilkens for the generous gift of purified yeast V_o complexes.

REFERENCES

Amberg DC, Burke DJ, Strathern JN (2005). Methods in Yeast Genetics, Cold Spring Harbor, NY: Cold Spring Harbor Laboratory Press.

Baskaran S, Ragusa MJ, Boura E, Hurley JH (2012). Two-site recognition of phosphatidylinositol 3-phosphate by PROPPINs in autophagy. Mol Cell 47, 339–348.

Batelli G, Verslues PE, Agius F, Qiu Q, Fujii H, Pan S, Schumaker KS, Grillo S, Zhu JK (2007). SOS2 promotes salt tolerance in part by interacting with the vacuolar H+-ATPase and upregulating its transport activity. Mol Cell Biol 27, 7781–7790.

Benlekbir S, Bueler SA, Rubinstein JL (2012). Structure of the vacuolar-type ATPase from *Saccharomyces cerevisiae* at 11-A resolution. Nat Struct Mol Biol 19, 1356–1362.

Bolte S, Cordelieres FP (2006). A guided tour into subcellular colocalization analysis in light microscopy. J Microsc 224, 213–232.

Bonangelino CJ, Nau JJ, Duex JE, Brinkman M, Wurmser AE, Gary JD, Emr SD, Weisman LS (2002). Osmotic stress-induced increase of phosphatidylinositol 3,5-bisphosphate requires Vac14p, an activator of the lipid kinase Fab1p. J Cell Biol 156, 1015–1028.

Botelho RJ, Efe JA, Teis D, Emr SD (2008). Assembly of a Fab1 phosphoinositide kinase signaling complex requires the Fig4 phosphoinositide phosphatase. Mol Biol Cell 19, 4273–4286.

Chow CY *et al*. (2007). Mutation of FIG4 causes neurodegeneration in the pale tremor mouse and patients with CMT4J. Nature 448, 68–72.

Chow CY *et al*. (2009). Deleterious variants of FIG4, a phosphoinositide phosphatase, in patients with ALS. Am J Hum Genet 84, 85–88.

Cooke FT, Dove SK, McEwen RK, Painter G, Holmes AB, Hall MN, Michell RH, Parker PJ (1998). The stress-activated phosphatidylinositol 3-phosphate 5-kinase Fab1p is essential for vacuole function in S. cerevisiae. Curr Biol 8, 1219–1222.

De Camilli P, Emr SD, McPherson PS, Novick P (1996). Phosphoinositides as regulators in membrane traffic. Science 271, 1533–1539.

Diakov TT, Kane PM (2010). Regulation of vacuolar proton-translocating ATPase activity and assembly by extracellular pH. J Biol Chem 285, 23771–23778.

Diepholz M, Venzke D, Prinz S, Batisse C, Florchinger B, Rossle M, Svergun DI, Bottcher B, Fethiere J (2008). A different conformation for EGC stator subcomplex in solution and in the assembled yeast V-ATPase: possible implications for regulatory disassembly. Structure 16, 1789–1798.

Di Paolo G, De Camilli P (2006). Phosphoinositides in cell regulation and membrane dynamics. Nature 443, 651–657.

Doherty RD, Kane PM (1993). Partial assembly of the yeast vacuolar H(+)-ATPase in mutants lacking one subunit of the enzyme. J Biol Chem 268, 16845–16851.

Dong XP *et al*. (2010). PI(3,5)P(2) controls membrane traffic by direct activation of mucolipin ca release channels in the endolysosome. Nat Commun 1, 38.

Dove SK, Cooke FT, Douglas MR, Sayers LG, Parker PJ, Michell RH (1997). Osmotic stress activates phosphatidylinositol-3,5-bisphosphate synthesis. Nature 390, 187–192.

Dove SK, McEwen RK, Cooke FT, Parker PJ, Michell RH (1999). Phosphatidylinositol 3,5-bisphosphate: a novel lipid that links stress responses to membrane trafficking events. Biochem Soc Trans 27, 674–677.

Dove SK, McEwen RK, Mayes A, Hughes DC, Beggs JD, Michell RH (2002). Vac14 controls PtdIns(3,5)P(2) synthesis and Fab1-dependent protein trafficking to the multivesicular body. Curr Biol 12, 885–893.

Duex JE, Nau JJ, Kauffman EJ, Weisman LS (2006a). Phosphoinositide 5-phosphatase Fig 4p is required for both acute rise and subsequent fall in stress-induced phosphatidylinositol 3,5-bisphosphate levels. Eukaryot Cell 5, 723–731.

Duex JE, Tang F, Weisman LS (2006b). The Vac14p-Fig4p complex acts independently of Vac7p and couples PI3,5P2 synthesis and turnover. J Cell Biol 172, 693–704.

Ferguson CJ, Lenk GM, Meisler MH (2009). Defective autophagy in neurons and astrocytes from mice deficient in PI(3,5)P2. Hum Mol Genet 18, 4868–4878.

Finnigan GC, Cronan GE, Park HJ, Srinivasan S, Quiocho FA, Stevens TH (2012). Sorting of the yeast vacuolar-type, proton-translocating ATPase enzyme complex (V-ATPase): identification of a necessary and sufficient Golgi/endosomal retention signal in Stv1p. J Biol Chem 287, 19487–19500.

Forgac M (2007). Vacuolar ATPases: rotary proton pumps in physiology and pathophysiology. Nat Rev Mol Cell Biol 8, 917–929.

Gary JD, Sato TK, Stefan CJ, Bonangelino CJ, Weisman LS, Emr SD (2002). Regulation of Fab1 phosphatidylinositol 3-phosphate 5-kinase pathway by Vac7 protein and Fig4, a polyphosphoinositide phosphatase family member. Mol Biol Cell 13, 1238–1251.

Gary JD, Wurmser AE, Bonangelino CJ, Weisman LS, Emr SD (1998). Fab1p is essential for PtdIns(3)P 5-kinase activity and the maintenance of vacuolar size and membrane homeostasis. J Cell Biol 143, 65–79.

Hayakawa A, Hayes SJ, Lawe DC, Sudharshan E, Tuft R, Fogarty K, Lambright D, Corvera S (2004). Structural basis for endosomal targeting by FYVE domains. J Biol Chem 279, 5958–5966.

Hilgemann DW (2007). On the physiological roles of PIP(2) at cardiac Na+ Ca2+ exchangers and K(ATP) channels: a long journey from membrane biophysics into cell biology. J Physiol 582, 903–909.

Ho CY, Alghamdi TA, Botelho RJ (2012). Phosphatidylinositol-3,5-bisphosphate: no longer the poor PIP2. Traffic 13, 1–8.

Ikonomov OC, Sbrissa D, Delvecchio K, Xie Y, Jin JP, Rappolee D, Shisheva A (2011). The phosphoinositide kinase PIKfyve is vital in early embryonic development: preimplantation lethality of PIKfyve-/- embryos but normality of PIKfyve+/- mice. J Biol Chem 286, 13404–13413.

Ikonomov OC, Sbrissa D, Foti M, Carpentier JL, Shisheva A (2003). PIKfyve controls fluid phase endocytosis but not recycling/degradation of endocytosed receptors or sorting of procathepsin D by regulating multivesicular body morphogenesis. Mol Biol Cell 14, 4581–4591.

Jin N *et al*. (2008). VAC14 nucleates a protein complex essential for the acute interconversion of PI3P and PI(3,5)P(2) in yeast and mouse. EMBO J 27, 3221–3234.

Kane PM (1995). Disassembly and reassembly of the yeast vacuolar H(+)-ATPase in vivo. J Biol Chem 270, 17025–17032.

Kane PM (2006). The where, when, and how of organelle acidification by the yeast vacuolar H+-ATPase. Microbiol Mol Biol Rev 70, 177–191.

Kane PM, Kuehn MC, Howald-Stevenson I, Stevens TH (1992). Assembly and targeting of peripheral and integral membrane subunits of the yeast vacuolar H(+)-ATPase. J Biol Chem 267, 447–454.

Kawasaki-Nishi S, Bowers K, Nishi T, Forgac M, Stevens TH (2001). The amino-terminal domain of the vacuolar proton-translocating ATPase a subunit controls targeting and in vivo dissociation, and the carboxyl-terminal domain affects coupling of proton transport and ATP hydrolysis. J Biol Chem 276, 47411–47420.

Keenan Curtis K, Kane PM (2002). Novel vacuolar H+-ATPase complexes resulting from overproduction of Vma5p and Vma13p. J Biol Chem 277, 2716–2724.

Lemmon MA (2008). Membrane recognition by phospholipid-binding domains. Nat Rev Mol Cell Biol 9, 99–111.

Li SC, Diakov TT, Rizzo JM, Kane PM (2012). Vacuolar H+-ATPase works in parallel with the HOG pathway to adapt *Saccharomyces cerevisiae* cells to osmotic stress. Eukaryot Cell 11, 282–291.

Lin M, Li SC, Kane PM, Hofken T (2012). Regulation of vacuolar H+-ATPase activity by the Cdc42 effector Ste20 in *Saccharomyces cerevisiae*. Eukaryot Cell 11, 442–451.

Liu M, Tarsio M, Charsky CM, Kane PM (2005). Structural and functional separation of the N-and C-terminal domains of the yeast V-ATPase subunit H. J Biol Chem 280, 36978–36985.

Longtine MS, McKenzie A 3rd, Demarini DJ, Shah NG, Wach A, Brachat A, Philippsen P, Pringle JR (1998). Additional modules for versatile and economical PCR-based gene deletion and modification in *Saccharomyces cerevisiae*. Yeast 14, 953–961.

Manolson MF, Proteau D, Preston RA, Stenbit A, Roberts BT, Hoyt MA, Preuss D, Mulholland J, Botstein D, Jones EW (1992). The VPH1 gene encodes a 95-kDa integral membrane polypeptide required for in vivo assembly and activity of the yeast vacuolar H(+)-ATPase. J Biol Chem 267, 14294–14303.

Mollapour M, Phelan JP, Millson SH, Piper PW, Cooke FT (2006). Weak acid and alkali stress regulate phosphatidylinositol bisphosphate synthesis in *Saccharomyces cerevisiae*. Biochem J 395, 73–80.
Muench SP, Huss M, Song CF, Phillips C, Wieczorek H, Trinick J, Harrison MA (2009). Cryo-electron microscopy of the vacuolar ATPase motor reveals its mechanical and regulatory complexity. J Mol Biol 386, 989–999.
Nicot AS, Fares H, Payrastre B, Chisholm AD, Labouesse M, Laporte J (2006). The phosphoinositide kinase PIKfyve/Fab1p regulates terminal lysosome maturation in *Caenorhabditis elegans*. Mol Biol Cell 17, 3062–3074.
Oot RA, Wilkens S (2010). Domain characterization and interaction of the yeast vacuolar ATPase subunit C with the peripheral stator stalk subunits E and G. J Biol Chem 285, 24654–24664.
Oot RA, Wilkens S (2012). Subunit interactions at the V1-Vo interface in yeast vacuolar ATPase. J Biol Chem 287, 13396–13406.
Parra KJ, Keenan KL, Kane PM (2000). The H subunit (Vma13p) of the yeast V-ATPase inhibits the ATPase activity of cytosolic V1 complexes. J Biol Chem 275, 21761–21767.
Qi J, Forgac M (2008). Function and subunit interactions of the N-terminal domain of subunit a (Vph1p) of the yeast V-ATPase. J Biol Chem 283, 19274–19282.
Queiros F, Fontes N, Silva P, Almeida D, Maeshima M, Geros H, Fidalgo F (2009). Activity of tonoplast proton pumps and Na+/H+ exchange in potato cell cultures is modulated by salt. J Exp Bot 60, 1363–1374.
Rahman S *et al*. (2013). Biochemical and biophysical properties of interactions between subunits of the peripheral stalk region of human V-ATPase. PLoS One 8, e55704.
Roberts CJ, Raymond CK, Yamashiro CT, Stevens TH (1991). Methods for studying the yeast vacuole. Methods Enzymol 194, 644–661.
Roth MG (2004). Phosphoinositides in constitutive membrane traffic. Physiol Rev 84, 699–730.
Rudge SA, Anderson DM, Emr SD (2004). Vacuole size control: regulation of PtdIns(3,5)P_2 levels by the vacuole-associated Vac14-Fig4 complex, a PtdIns(3,5)P_2-specific phosphatase. Mol Biol Cell 15, 24–36.
Rusten TE, Rodahl LM, Pattni K, Englund C, Samakovlis C, Dove S, Brech A, Stenmark H (2006). Fab1 phosphatidylinositol 3-phosphate 5-kinase controls trafficking but not silencing of endocytosed receptors. Mol Biol Cell 17, 3989–4001.
Sambade M, Alba M, Smardon AM, West RW, Kane PM (2005). A genomic screen for yeast vacuolar membrane ATPase mutants. Genetics 170, 1539–1551.
Shisheva A (2012). PIKfyve and its lipid products in health and in sickness. Curr Top Microbiol Immunol 362, 127–162.
Silva P, Geros H (2009). Regulation by salt of vacuolar H+-ATPase and H+-pyrophosphatase activities and Na+/H +exchange. Plant Signal Behav 4, 718–726.
Smardon AM, Kane PM (2007). RAVE is essential for the efficient assembly of the C subunit with the vacuolar H(+)-ATPase. J Biol Chem 282, 26185–26194.
Srinivasan S, Vyas NK, Baker ML, Quiocho FA (2011). Crystal structure of the cytoplasmic N-terminal domain of subunit I, a homolog of subunit a, of V-ATPase. J Mol Biol 412, 14–21.
Strahl T, Thorner J (2007). Synthesis and function of membrane phosphoinositides in budding yeast, *Saccharomyces cerevisiae*. Biochim Biophys Acta 1771, 353–404.
Suh BC, Hille B (2005). Regulation of ion channels by phosphatidylinositol 4,5-bisphosphate. Curr Opin Neurobiol 15, 370–378.
Suh BC, Hille B (2008). PIP2 is a necessary cofactor for ion channel function: how and why? Annu Rev Biophys 37, 175–195.
Takasuga S *et al*. (2013). Critical roles of type III phosphatidylinositol phosphate kinase in murine embryonic visceral endoderm and adult intestine. Proc Natl Acad Sci USA 110, 1726–1731.
Tamura N, Oku M, Ito M, Noda NN, Inagaki F, Sakai Y (2013). Atg18 phosphoregulation controls organellar dynamics by modulating its phosphoinositide-binding activity. J Cell Biol 202, 685–698.
Voss M, Vitavska O, Walz B, Wieczorek H, Baumann O (2007). Stimulus-induced phosphorylation of vacuolar H(+)-ATPase by protein kinase A. J Biol Chem 282, 33735–33742.
Walls KC, Ghosh AP, Franklin AV, Klocke BJ, Ballestas M, Shacka JJ, Zhang J, Roth KA (2010). Lysosome dysfunction triggers Atg7-dependent neural apoptosis. J Biol Chem 285, 10497–10507.
Wilkens S, Forgac M (2001). Three-dimensional structure of the vacuolar ATPase proton channel by electron microscopy. J Biol Chem 276, 44064–44068.
Yamashiro CT, Kane PM, Wolczyk DF, Preston RA, Stevens TH (1990). Role of vacuolar acidification in protein sorting and zymogen activation: a genetic analysis of the yeast vacuolar proton-translocating ATPase. Mol Cell Biol 10, 3737–3749.
Yan Y, Denef N, Schupbach T (2009). The vacuolar proton pump, V-ATPase, is required for notch signaling and endosomal trafficking in *Drosophila*. Dev Cell 17, 387–402.
Young BP *et al*. (2010). Phosphatidic acid is a pH biosensor that links membrane biogenesis to metabolism. Science 329, 1085–1088.
Zhang X, Chow CY, Sahenk Z, Shy ME, Meisler MH, Li J (2008a). Mutation of FIG4 causes a rapidly progressive, asymmetric neuronal degeneration. Brain 131, 1990–2001.
Zhang Y *et al*. (2007). Loss of Vac14, a regulator of the signaling lipid phosphatidylinositol 3,5-bisphosphate, results in neurodegeneration in mice. Proc Natl Acad Sci USA 104, 17518–17523.
Zhang Z, Zheng Y, Mazon H, Milgrom E, Kitagawa N, Kish-Trier E, Heck AJ, Kane PM, Wilkens S (2008b). Structure of the yeast vacuolar ATPase. J Biol Chem 283, 35983–35995.